A new noise erosion operator for anisotropic diffusion

Chao Cai (蔡 超), Mingyue Ding (丁名跃), Chengping Zhou (周成平), and Tianxu Zhang (张天序)

Institute for Pattern Recognition and Artificial Intelligence, State Education Commission Key Lab for Image Processing and Intelligent Control, Huazhong University of Science and Technology, Wuhan 430074

Received December 24, 2003

A noise erosion operator based on partial differential equation (PDE) is introduced, which has an excellent ability of noise removal and edge preservation for two-dimensional (2D) gradient data. The operator is applied to estimate a new diffusion coefficient. Experimental results demonstrate that anisotropic diffusion based on this new erosion operator can efficiently reduce noise and sharpen object boundaries.

OCIS codes: 100.2000, 120.2440, 170.3010, 290.1990.

In many applications, it is necessary to smooth an image while preserving its edges. However, linear filtering techniques often introduce edges blurring. Perona and Malik introduced an elegant formulation of anisotropic diffusion[1]. In their formulation, the image is considered as a medium where a fluid can diffuse in an anisotropic manner. Gerig and Kübler *et al.* early used anisotropic diffusion in magnetic resonance image (MRI) filtering[2].

The success of anisotropic diffusion based noise removal approach is greatly dependent on the estimation of diffusion coefficient. Nowadays, many diffusion approaches have been developed[1−4]. Among them, the diffusion coefficient is taken as a function of local image gradient, which determines how to diffuse a point in the image. However, the use of gradient may produce some difficulties, such as the failure to remove high contrast noise. The first coefficient estimation capable to increase the scale of the gradient was proposed by Catté *et al.*[3], they smoothed the input image firstly. This scheme evaluated the diffusion coefficient from a smoothed lower resolution image. Therefore edge shift is unavoidable, which is obviously conflicted to the motivation that people use anisotropic diffusion.

Segall and Acton suggested incorporating morphological operators into the diffusion coefficient[4]. But how to design a structural element adapted to different image structures is open. In this paper, we introduce a partial differential equation (PDE) based morphological erosion operator, which can be used in gradient image directly. The new diffusion coefficient implementation is robust to noise with a good localization of edges.

Anisotropic diffusion equation comes from a modified heat diffusion equation, i.e.

$$\frac{\partial u}{\partial t} = \mathrm{div}(c \cdot \nabla u), \tag{1}$$

where "div" is the divergence operator, ∇u is the image gradient, and c is the spatially varying diffusion coefficient. A standard diffusion coefficient is defined as

$$c = \mathrm{e}^{-\left(\frac{\|\nabla u\|}{\lambda}\right)^2}, \tag{2}$$

where λ is the gradient threshold determining the preserved edge magnitude.

As mentioned above, pre-smoothing of input image will produce edge shift. To solve this problem, we need to smooth gradient image directly with morphological operation. One of the most important issues in morphological operation is to determine an appropriate structural element. If choosing a fixed structural element, the minimizing rule of erosion operation often prevents the image from keeping the fine edge. In order to alleviate this problem, a dynamic structural element adapted to data's structures has to be applied. Because edge of image can be considered as linear pattern in its gradient image, we use PDE to derive our new erosion operator.

Let $f : R^d \to R$ be a function of n-dimensional signal ($n = 1, 2, 3, \cdots$). B is a disc with a radius t centered in (0, 0), e.g., $B = \{(x, y) : \sqrt{x^2 + y^2} \le t\}$, where t is a constant. Continuous-scale dilation or erosion of f by B is the solution of the following PDE with the initial condition f

$$\partial_t u = \pm |\nabla u| . \tag{3}$$

Different numerical approximations of Eq. (3) may derive different PDE-based morphological dilation or erosion operators. For instance, Osher and Sethian presented a simplest four-neighbor numerical approximation scheme (upwind scheme) of Eq. (3) in Ref. [5]. Similar to their approach, we extend the upwind gradient strength based operation $\varepsilon(u_{ij})$ to 8 neighbors

$$\begin{aligned}\varepsilon(u_{ij}) = -\Big\{&[\min((u_{i-1\,j} - u_{ij})/h_1, 0)]^2 \\ &+ [\min((u_{i+1\,j} - u_{ij})/h_1, 0)]^2 \\ &+ [\min((u_{ij-1} - u_{ij})/h_2, 0)]^2 \\ &+ [\min((u_{ij+1} - u_{ij})/h_2, 0)]^2 \\ &+ [\min((u_{i-1\,j-1} - u_{ij})/h_3, 0)]^2 \\ &+ [\min((u_{i+1\,j+1} - u_{ij})/h_3, 0)]^2 \\ &+ [\min((u_{i+1\,j-1} - u_{ij})/h_4, 0)]^2 \\ &+ [\min((u_{i-1j+1} - u_{ij})/h_4, 0)]^2\Big\}^{1/2},\end{aligned}$$

where $h_k (k = 1, 2, 3, 4)$ is the distance between two neighbors. Using this definition, a new noise erosion operator

is given by

$$u_{ij}^{n+1} = E(u_{ij}^n)$$

$$= \min(k_1 \max(u_{ij}^n + k_2\varepsilon(u_{ij}^n), u_{\min}), u_{\max}), \quad (4)$$

where k_1 and k_2 are constants, $u_{\min}$ and $u_{\max}$ are the minimum and maximum of u^0. Supposing the background of image u is zero, from Eq. (4), it is clear that by properly choosing the values of k_1 and k_2, the isolated positive pulses can be removed while the positive linear structures are remained. Thus, the isolated bright noise points in image are eroded while the bright edges are left. For gradient image, we split it into two parts: $u_{ij}^n = (u_{ij}^n)^+ - (u_{ij}^n)^-$ (here $(u_{ij}^n)^+ = \max(u_{ij}^n, 0)$ and $(u_{ij}^n)^- = -\min(u_{ij}^n, 0)$). The eroding of u_{ij}^n becomes

$$u_{ij}^{n+1} = \hat{E}(u_{ij}^n) = E((u_{ij}^n)^+) - E((u_{ij}^n)^-). \quad (5)$$

The new edge preserved diffusion coefficient can be implemented through eroding the gradient data, $\nabla_i u_t$, that is

$$c = \mathrm{e}^{-\left(\frac{\|\hat{E}(\nabla_i u_t)\|}{\lambda}\right)^2}, \quad (6)$$

where $\hat{E}(\cdot)$ denotes the noise erosion operator given in Eq. (5). If necessary, the eroding operation will repeat in each diffusion step. Our experiments showed that once or twice is usually enough even for lower signal to noise ratio (SNR) image.

There are two points have to be pointed out. 1) The new erosion operator only works well for the image with zero background such as gradient image. Its ideal input is the difference of piecewise-constant image. 2) Different from other filters such as median filter, this erosion operator does not introduce edge's blurring. The latter property makes it able to efficiently suppress image noise and perfectly preserve the edges of image.

Let $h_1 = h_2 = h_3 = h_4 = 1$, $k_1 = 2(2 + \sqrt{3})$, and $k_2 = \sqrt{2}/4$, we performed our experiments.

In the first experiment, we chose a synthesize image (Fig. 1(a)). The eroding result is shown in Fig. 1(b). From Fig. 1, it is demonstrated that our erosion operator results in good noise erosion for zero background noise image.

In the second experiment, the eight-direction digitized form of the anisotropic diffusion equation (Eq. (1)) was used. Figure 2 shows the comparison of the diffusion approach based on our erosion operator, Catté diffusion[3], and the conventional morphological diffusion in Ref. [4]

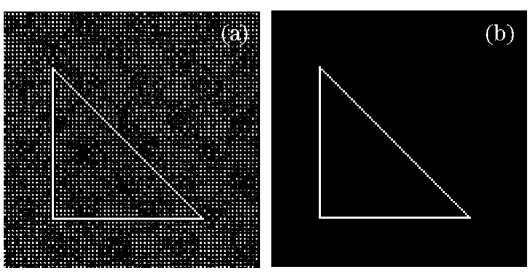

Fig. 1. New morphological erosion result on a synthesize image. (a) Noise image, (b) eroding result of (a) with the operator given in Eq. (5).

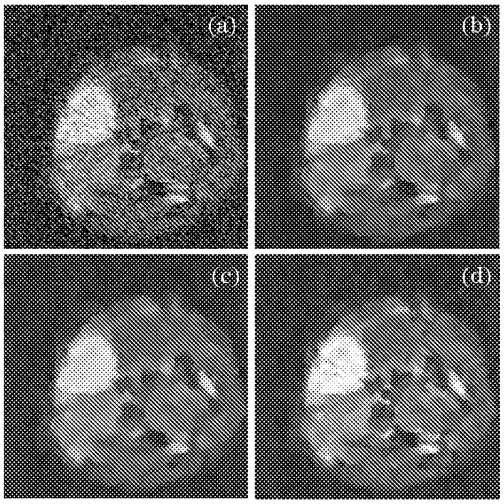

Fig. 2. Comparison of two conventional approaches and our diffusion scheme for a rat head MR image. (a) Original rat MRI, (b) image after Catté diffusion filtering ($\lambda = 0.15\sigma_n$), (c) image after close-open diffusion filtering ($\lambda = 0.15\sigma_n$), and (d) image after our diffusion filtering ($\lambda = 0.2\sigma_n$).

Table 1. SNR Comparison of Diffusion Based on our Noise Erosion Operator and other Three Conventional Diffusion Approaches. The First Column Lists the SNR of the Input Images (Unit: dB)

Elaine	Perona	Catté	Close-Open	This Paper
1.62	11.16	12.89	13.26	13.31
3.30	12.23	13.68	14.27	14.36
4.31	12.77	14.12	14.86	14.92
6.34	13.94	14.98	15.91	16.08
8.99	15.31	16.18	17.18	17.39

with a rat head MRI (Fig. 2(a)). The rat head MRI was captured on a 4.7-T MRI imaging system at Wuhan Physics and Mathematics Institute (3500-ms repetition time (TR), 50-ms echo time (TE), 3.0-cm field of view (FOV), 1.00-mm slice thickness). Ten iterations were executed for each filtering approach. The noise variance in MRI is estimated using the method described in Ref. [6]. Table 1 lists the Perona diffusion ($\lambda = 1.2\sigma_n$)[1], Catté diffusion, morphological diffusion, and our filtering results of standard Elaine picture added by the Gaussian white noise. From the experiment, it was demonstrated that our operator could efficiently suppress the noise and perfectly preserve the edge structures, especially the fine details of edges. The SNR of our filtered image is much higher than others.

In this paper, we proposed a noise erosion operator by using PDE. It has excellent abilities in both noise erosion and edge preservation for gradient image. Experiment results with different images demonstrated that the diffusion based on the new erosion operator overcomes the drawbacks of other approaches such as edge shift. One of the problems in our operator is its time-consuming computation that we are working on. The

other future work includes to apply the idea in other applications such as edge extraction.

This work was supported by the National Natural Science Foundation of China under Grant No. 60135020 F F030405. C. Cai's e-mail address is caichao@mail.hust.edu.cn.

References

1. P. Perona and J. Malik, IEEE Trans. Pattern Anal. Machine Intell. **12,** 629 (1990).
2. G. Gerig, O. Kübler, R. Kikinis, and F. A. Jolesz, IEEE Trans. Medical Imaging **11,** 221 (1992).
3. F. Catté, P. L. Lions, J. M. Morel, and T. Coll, SIAM J. Numerical Analysis **29,** 182 (1992).
4. C. A. Segall and S. T. Acton, in *Proceedings of International Conference on Image Processing* **3,** 348 (1997).
5. S. Osher and J. A. Sethian, Computational Physics **79,** 12 (1988).
6. J. Immerker, Computer Vision and Image Understanding **64,** 300 (1996).